SPE
Society of Petroleum Engineers

SPE 20058

Subsidence-Induced Well Failure

M.S. Bruno, Chevron Oil Field Research Co.

This paper was prepared for presentation at the 60th California Regional Meeting held in Ventura, California, April 4-6, 1990.

ABSTRACT

The withdrawal of fluids from a reservoir can sometimes produce significant formation compaction and surface subsidence. In extreme instances hundreds of well casings have been seriously damaged and offshore platforms have partially submerged. The largest displacements caused by subsidence occur in the vertical direction, as indicated by analytic and numerical studies, and confirmed with field surveys. However, a significant number of well failures observed in the field are not caused by compression or buckling due to maximum vertical deformation of the formation center, but are instead related to shear and bending deformation.

In this paper, analytic and numerical models are first reviewed to describe surface and subsurface elastic deformation due to subsidence. Rock and structural mechanics principles are then applied to analyze potential well failure mechanisms, including axial compression, buckling, shear and bending modes. Maximum compressional strains develop within the producing formation near the reservoir center. Maximum shear and bending deformations, however, develop within the overburden material above the reservoir flanks. Well failures are very often associated with subsidence induced shear bedding slip or fault movement in these zones. Simple models describing these failure processes are also presented and compared with field observation.

INTRODUCTION

The weight of overburden sediments above a producing formation is supported partially by the rock matrix and partially by the pressurized fluid within the rock porespace. When fluid pressure is reduced, more of the load is transferred to the rock matrix and the formation is compacted. This subsurface compaction can sometimes also produce surface subsidence, with significant displacements in both the vertical and horizontal directions. When significant subsidence does occur, it can result in serious financial and environmental impact.

For example, from about 1935 to 1965 the surface above the Wilmington oil field in California subsided almost 10m. The costs to elevate, protect, and repair various facilities exceeded $100 million by 1962.[1] The subsidence caused casing failure in several hundred wells. More recently, by 1987 about 4m of seafloor subsidence was measured above the Ekofisk gas field in the North Sea.[2] The entire project to raise platforms and protect storage facilities at this important offshore complex exceeded $400 million.[3] Casing failures have occured in more than two-thirds of the wells.[4]

Several researchers have described some of the effects of compaction and subsidence on well casing compression and buckling failure, including Wilson et. al.,[5] Bradley and Chia,[6] and Yudovich et. al.[4] But these studies have not considered well failure associated with shear and bending deformations. The purpose of this paper is to analyze a wider range of potential well failure mechanisms, to describe the locations for these failures, and to compare analytical and numerical model results with field observations.

SUBSIDENCE INDUCED RESERVOIR DISPLACEMENTS

When the lateral dimensions of the reservoir are very large compared to its vertical thickness, most of the subsurface compression associated with fluid withdrawal can be assumed to occur in the vertical direction. The vertical compaction, dH, of a reservoir may then be defined with the following expression:

$$dH/H = C_m dP, \qquad (1)$$

where H is the original reservoir thickness, C_m is the uniaxial compaction coefficent of the material, and dP is the change in reservoir pressure.

Subsidence refers to the surface displacement that may be produced by subsurface reservoir compaction. The degree to which this subsurface compaction is transferred to surface displacement depends on the areal extent of the reservoir and the depth of burial. A large shallow reservoir, for example, will produce much more extensive surface subsidence than a small deeply buried one with identical material properties and pressure drawdown.

Analytic Solution

Surface displacements resulting from subsurface compaction may be obtained by applying the nucleus of strain concept from continuum mechanics, described by J. Geertsma in 1973.[7-8] The volumetric strain at a point, caused by a local reduction in prore pressure, is treated as a center of compression in an elastic half space. This produces a corresponding displacement at the free surface. The total surface deformation caused by a varying pressure reduction within an arbitrarily shaped reservoir is then given by integrating the contribution of all these compression points over the reservoir volume as follows:

$$U_x(x_o,y_o) = -\frac{C_m}{\pi}(1-\nu)\int_V \frac{x_o - x}{((x-x_o)^2+(y-y_o)^2+z^2)^{\frac{3}{2}}}\Delta P(x,y,z)dV. \quad (2)$$

$$U_y(x_o,y_o) = -\frac{C_m}{\pi}(1-\nu)\int_V \frac{y_o - y}{((x-x_o)^2+(y-y_o)^2+z^2)^{\frac{3}{2}}}\Delta P(x,y,z)dV. \quad (3)$$

$$U_z(x_o,y_o) = \frac{C_m}{\pi}(1-\nu)\int_V \frac{z}{((x-x_o)^2+(y-y_o)^2+z^2)^{\frac{3}{2}}}\Delta P(x,y,z)dV. \quad (4)$$

In the expressions above U_x and U_y are the horizontal displacements and U_z is the vertical displacement at position (X_o, Y_o, Z_o) on the surface as shown in Figure 1. $\Delta P(x,y,z)$ defines the pressure drawdown within the reservoir volume, V. The Poisson ratio for the material, ν, relates the horizontal expansion to the vertical load. Except for a few cases, these equations are difficult to solve analytically, but can be easily calculated with summation or numerical integration techniques on a PC.

Equation (4) can be greatly simplified if the reservoir is roughly disk shaped, with average radius R, thickness H, and and burial depth, D, at the top of the formation. Above the center of a reservoir with uniform pressure drawdown, ΔP, the expression for maximum vertical subsidence reduces to:

$$max\ U_z = 2C_m(1-\nu)\Delta P\left(H - \sqrt{R^2+(D+H)^2} + \sqrt{R^2+D^2}\right). \quad (5)$$

The displacement pattern for a disk shaped reservoir, with depth of burial equal to its radial size, subject to uniform pressure drawdown is presented in Figure 2. The vertical surface subsidence is maximum at the center and falls off to a value less than 20 percent of maximum at a distance about twice the reservoir radius away. The horizontal displacement exceeds 40 percent of the maximum vertical subsidence near the reservoir edge, where the vertical subsidence gradient is steepest.

Finite Element Analysis

The analytic solutions presented above are simple to apply and can provide reasonable estimates for surface displacements above reservoirs with uniform material properties. Unfortunately, the analytic expressions provide displacement information only at the surface, not throughout the entire vertical section.

Finite element methods may be applied to provide more complete information for a wider range of reservoir geometries and pressure conditions. In addition, the effects of compaction and subsidence on well casings and surface structures may also be assessed. Predictions of subsurface deformation throughout the field may sometimes be applied to help optimize the location and trajectory of wells planned for subsiding reservoirs.

With the finite element method, the entire reservoir is partitioned into a number of discrete small blocks, or elements, as illustrated schematically in Figure 3. Material properties may vary throughout the volume. Variational energy principles are applied to relate global displacements to element deformations caused by changes in pore fluid pressure. The level of complexity may vary from simple two dimensional approximations (assuming radial or longitudinal symmetry within the field) to full three dimensional models with time varying pressure distributions and non-linear material properties.

As an illustrative example, consider the two-dimensional finite element model for subsidence over a relatively shallow, thick, reservoir with properties summarized in Table 1. This analysis was performed using the ADINA finite element code. Pressure drawdown and field deformations are assumed to be symmetric about the reservoir center. Vertical wells of 7-in. casing diameter are located at several horizontal positions. The resulting deformation pattern is shown in Figure 4, with vertical exaggeration. Also indicated are approximate positions of maximum compression, shear, and bending stresses on wells.

WELL FAILURE MECHANISMS

Casing Compression and Buckling

Compression and buckling of wells may be caused by large vertical deformation. Consider a typical cement and casing completion depicted in Figure 5. As the formation compacts due to pore pressure reduction, loads are transferred from the formation to the cement and finally to the casing. The well casing may fail due to compressive yielding or buckling. The cement may also be damaged due to high shear and compressive stresses.

The most likely location for casing compression failure is near the center of the producing interval, where the vertical strain is largest. If no slip occurs between the formation and cement and between the cement and casing, then the maximum axial strain, Σ_{zz}, in the casing can be approximated by the total compaction of the producing interval. Assuming most of the reservoir deformation occurs in the vertical direction, and that the

formation compressibility is constant, the axial strain can be approximated by:

$$\varepsilon_{zz} = \frac{\Delta H}{H} = C_m \Delta P. \quad (6)$$

Critical strains for casing steel range from about 0.3% to 0.7%, depending on the grade. Using the lower value as a conservative estimate, the critical pressure drawdown necessary to produce compressive failure in the casing can be approximated as:

$$\Delta P_{cr} \approx \frac{0.003}{C_m}. \quad (7)$$

The expression for critical drawdown given above is very conservative because it is based on the assumption that the amount of casing shortening is equal to the total formation compaction. Shear slip often occurs at the interface between the formation and cement or between the cement and casing. This is particularly true for unconsolidated sands. Collar logs in the field usually indicate that vertical casing strain is less than the measured formation compaction. In the Wilmington field, for example, measured axial casing strain was less than ten percent of the total formation compaction. In extreme instances at other locations, wellheads have actually been left protruding in the air after the surface subsided.[9]

Casing Buckling Failure

Casing instability, or buckling, may occur if the axial load becomes large and there is insufficient lateral restraint provided by the formation. As with compressive failure, the most likely location for this problem will be near the center of the producing formation where the vertical strain is maximum. A conservative estimate for minimum buckling load can be obtained by again assuming no slip at the casing interfaces and relating the axial force to the compaction strain.

$$F_z = A_c E_c \varepsilon_{zz} = A_c E_c C_m \Delta P \quad (8)$$

In the equation above, A_c is the casing cross sectional area and E_c is the casing material Young's Modulus. A further conservative assumption is that the casing is not rotationally constrained at the top and bottom of the production interval. Then equation (8) can be combined with a solution for the critical buckling force[10] to yield an expression for critical pressure drawdown.

$$\Delta P_{cr} = \frac{\pi^2 I}{A_c C_m L^2}\left(m^2 + \frac{\beta L^4}{m^2 \pi^4 E_c I}\right); \quad (m = 1,2,3...) \quad (9)$$

In the equation above, I is the casing moment of inertia and L is the length of casing within the producing interval. The term, β, represents the lateral formation stiffness and m defines the number of half sine waves into which the casing length will buckle at the minimum load. For example, when no restraint is supplied by the formation, $\beta = 0$. Then ΔP_{cr} will be a minimum when $m = 1$. This corresponds to the fundamental single half sine buckling mode. As β increases, the formation stiffness restricts lateral deformation and forces the well casing into higher order buckling modes with multiple sine waves.

The formation stiffness, β, has been related to the Young's Modulus for the formation, E_f, by Wilson and others.[5] In most practical situations the formation stiffness falls within the range:

$$2E_f < \beta < 5E_f. \quad (10)$$

The formation Young's Modulus is easily measured on core samples, and typical values range from 10 kpsi (69 MPa) for very soft sediments to 5,000 kpsi (34 GPa) for stiff, competent rock.

The critical drawdown pressure in equation (9) may be minimized with respect to m, to determine a critical buckling mode.

$$m_{cr}^2 = \sqrt{\frac{\beta L^4}{\pi^4 E_c I}} \quad (11)$$

The expression above is only approximate because m has been treated as a continuous, rather than integer variable. The equation becomes more accurate as the term within the square root becomes large compared to 1. Substituting equation (11) into (9) yields:

$$\Delta P_{cr} = \frac{2}{A_c C_m}\sqrt{\frac{\beta I}{E_c}}. \quad (12)$$

This expression suggests that only moderate formation stiffness is required to supress buckling failure, a result which has been supported experimentally.[5] In most situations, formation stiffness is sufficient to restrict buckling failure. One possible situation which can cause problems, however, is when a large vertical interval along the casing is very poorly cemented or has developed significant production-related cavities.

Casing Shear and Bending

The analysis provided above deals with failure caused by vertical deformations. Horizontal deformations can also cause casing failure through shear and bending. Such failure mechanisms have not been previously discussed in the literature. In the few cases where finite element analysis was performed,[4-6] a single well was placed at the center of an axisymmetric grid, so that only axial compression failure could be studied. Shear and bending well failures are actually more common and serious than compression and buckling failures for several reasons:

1. Lateral forces are applied directly to the well casing without the slip associated with vertical loading.

2. Bending strength of the cement layer around the casing is an order of magnitude lower than its compressive strength.

3. The deformed casing shape and location usually cause more severe production problems.

Shear and bending problems most often occur towards the flanks of the field and above the producing interval. As shown in Figure 2, this is the general area where the horizontal displacement magnitude and the vertical displacement gradient is maximum. While compression or buckling damage within the producing interval may have little obvious effect on productivity, well failure in the overburden (casing or tubing leak) is usually more serious, requiring major workover or abandonment.

Observations at several field have supported this general position for well failures. According to Poland and Davis,[9] shearing rupture destroyed several hundred well casings toward the flanks of the Wilmington oil field at depths around 1600 ft (488 m). (The producing interval started at about 2300 ft (701 m).) In the South Belridge field in California from 1984 to 1987, more than one hundred wells were damaged at depths around 750 ft (229 m). (The producing interval starts at about 1000 ft (305 m).) Well failures generally started on the east flank of the field and moved progressively inward.[11]

Although field evidence strongly suggests a primary failure mode is shear and bending, simple elastic mechanics theory alone cannot explain this phenomenon. For example, a worst-case estimate for shear, V, and bending moment, M, on a well casing can be determined from the maximum horizontal surface displacement, U_r. Assuming the well string is restrained from rotating at the surface and is completely fixed at the top of the producing interval, simple beam theory can be applied to obtain:

$$V = \frac{12EI}{L^3}U_r \; ; \; M = \frac{6EI}{L^2}U_r \, . \qquad (13)$$

Consider a 7-in. (18 cm) casing (E = 30,000 kpsi (207 GPa); I = 37in^4 (94cm^4)) from the surface to a producing interval 1000 feet (305 m) below, subjected to significant horizontal surface displacement, U_r = 8 ft (2.4 m). The shear force and bending moment predicted by equation (13) would be only 0.74 lb (3.3 N) and 4,440 in-lb (502 N-m), respectively. This is well below the casing strength capacity. If the well string rotates at the top or bottom, then even lower values of force would be predicted.

To explain widely-observed shear and bending failures in the field, the casings must be subjected to severe strain localization caused by large scale deformation of the overburden material. Non-elastic overburden deformation may result from material shear failure or a discontinuity in displacement (bedding slip or fault movement).

Overburden Shear Failure

Reservoir compaction produces high shear stresses in the overburden material near the flanks of the reservoir. For example, the solid lines shown in Figures 6 and 7 are calculated estimates of horizontal shear stress for the sample reservoir model described in Table 1, using the ADINA finite element model. Figure 6 presents the variation of shear stress with depth at a position about 1700 ft (518 m) from the reservoir center and Figure 7 presents the variation with lateral position at a depth of 700 feet (213 m).

Bedding layers of sand and clay are subject to shearing stresses caused by reservoir compaction and effective vertical stress due to the weight of overlying material minus pore pressure. Consider a simple Mohr-Coulomb failure criteria. The material is assumed to fail when the shear stress exceeds the material cohesive strength, S_o, plus the frictional restraint caused by the vertical stress:

$$\tau_{rz} \geq S_o + \mu\sigma_z \qquad (14)$$

In the expression above, μ represents the material coefficient of friction. For unconsolidated sediments, S_o is close to zero. Friction coefficients for sands are about 0.6 while friction coefficients for shale and clay can be as low as 0.25. Assuming a vertical stress gradient of about 1 psi/ft (0.023 MPa/m), approximate conservative failure lines for sand and clay may be expressed as:

$$\tau_{sand} \approx 0.6z \; ; \; \tau_{clay} \approx 0.25z \, . \qquad (15)$$

Clay zones or sand-clay interfaces are more likely to fail in shear than sand zones. The stress magnitude required for failure increases with depth and can be compared to numerically determined shear stresses in the overburden above a compacting formation, as shown in Figures 6 and 7 for the field model example. The dashed lines represent approximate failure criteria for shale and sand. It is seen that the subsidence-produced stress profile never exceeds the strength profile for sands but does exceed the strength profile for clays, with a maximum at about 800 feet (244 m).

This explanation for well failures is consistent with several field observations. For example more than twenty casing shear failures during 1983 at Chevron's Lost Hills field have been associated with movement along one or more bedding planes. A similar stress analysis by Lee[11] for the Wilmington field also matches observed shear failures of wells in the overburden zone.

The failure lines described above are only rough approximations. They do not take into account discontinuities in stress which can result from heterogeneous material bedding layers. More detailed failure limits may be incorporated within finite element material property definitions.

Subsidence-Induced Fault Movement

Previously we have described the formation as acting in a continuum manner. In some situations, however, a compacting reservoir can induce movement along faults within and above the producing formation. When the overburden structure is heavily faulted or fractured, it cannot provide adequate lateral support. More of the formations compaction

will be translated vertically into enhance surface subsidence adjacent to or between high angle faults.

The fault movement produces severe strain localization and will tend to shear well casings which cross the faults, as illustrated schematically in Figure 8. This type of mechanism was responsible for damage in more than 50 wells in the South Pass Block 27 oil field, offshore Louisiana,[13] and for several other well failures at the South Pass Block 78 field. Fault motion is usually gradual. But in several instances, fluid withdrawal has induced small-scale earthquakes up to Richter magnitude 3.5.[14] A very large number of well failures at Wilmington have been associated with instantaneous fault movement.

Since the lateral tectonic loads are usually unknown, the potential for subsidence-induced fault motion is difficult to assess. In general, longer and higher angle faults are most susceptible to induced motion. Faults across which pressure drawdown is non uniform are particularly prone to movement, especially when compaction occurs within the footwall block. The best course is to recognize and avoid these types of faults when selecting well locations and trajectories.

CONCLUSIONS

The following conclusions are supported by this study of subsidence induced well failure:

1. Subsidence can induce casing failure through several mechanisms, including compression, buckling, shear, and bending modes.

2. Finite element techniques may be applied to determine locations at which well failures are most likely, and can be used to help optimize well positions and inclinations.

3. While compression and buckling failures usually occur within the producing interval towards the center of the field, shear and bending failures often occur within the overburden structure above the flanks of the reservoir.

4. Field observations confirm that shear well failures within the overburden are not only very common, but are also generally more serious than compression or buckling failure within the producing interval.

5. A large number of shear casing failures are related to discontinuous deformation of the overburden material, including subsidence induced bedding plane slip and fault movement.

NOMENCLATURE

A_c = Casing Cross Section Area

β = Lateral Formation Stiffness

C_m = Uniaxial Compaction Coefficient

D = Reservoir Burial Depth

dH = Reservoir Compaction

dP = Change in Reservoir Pressure

Σ_{zz} = Vertical Strain Component

E_c = Casing Material Young's Modulus

E_f = Formation Material Young's Modulus

F_z = Casing Axial Force

L = Casing Length

M = Bending Movement

M_{cr} = Critical Buckling Mode

R = Average Reservoir Radius

r,z = Axisymmetric Coordinates

x,y,z = Cartesian Coordinates

U_x, U_y, U_z = Cartesian Surface Displacements

U_r, U_z = Axisymmetric Surface Displacements

ν = Poisson's Ratio

V = Reservoir Volume

τ_{rz} = Shear Stress Component

τ_{sand} = Sand Shear Limit

τ_{clay} = Clay Shear Limit

S_o = Material Cohesive Strength

ΔP_{cr} = Critical Drawdown Pressure

REFERENCES

1. Allen, D. R., "Subsidence Rebound and Surface Strain Associated With Oil Producing Operations, Long Beach, California," Assoc. Eng. Geol., Spec. Publ., 1973.

2. Sulak, R. M. and Danielsen, J., "Reservoir Aspects of Ekofisk Subsidence," Proc. Offshore Technology Conf. Houston, Texas, May 1988, OTC 5618 pp. 9-22.

3. Snyder, R. E. and McCabe, C. R., "Ekofisk Jack-up: The Story Behind the Headlines," Ocean Ind., Vol. 23, No 1., (Jan, 1988) pp 10.

4. Yudovich, A., Chin, L. Y., and Morgan, D. R., "Casing Deformation in Ekofisk," Proc. Offshore Technology Conf. Houston, Texas, May 1988, OTC 5623 pp. 63-72.

5. Wilson, W. N., Perkins, T. K., and Striegler, J. H., "Axial Buckling Stability of Cemented Pipe," Proc. 54th Conf. of the Soc. Pet. Eng. of AIME, Las Vegas, Nevada, Sept. 23-26, 1979. SPE 8254.

6. Bradley, D. A., and Chia, Y. P., "Evaluation of Reservoir Compaction and Its Effects on Casing Behavior," Proc. Deep Drilling and Production Symposium of the Soc. Pet. Eng. Amarillo, Texas, April 6-8, 1986. SPE 14985.

7. Geertsma, J., "Land Subsidence Above Compacting Oil and Gas Reservoirs," J. Pet. Tech., (June, 1973) pp. 734-744.

8. Geertsma, J., "A Numerical Technique for Predicting Subsidence Above Compacting Reservoirs, Based on the Nucleus of Strain Concept," Verhandelingen Kon. Ned. Geol. Mijnbouwk., vol. 28, 1973, pp. 63-78.

9. Poland, J. F. and Davis, G. H., "Land Subsidence Due to Withdrawal of Fluids" Reviews in Eng. Geology, Vol. II, (Geologic Society of America, Boulder, Co., 1969).

10. Timoshenko, S. P. and Gere, J. M., Theory of Elastic Stability, (McGraw Hill, New York, (2nd ed.) 1961).

11. Beatty, F. D., (Chevron USA, Western Region), personal communication Feb., 1989.

12. Lee, K. L., "Subsidence Earthquake at a California Oil Field," in Evaluation and Prediction of Subsidence, edited by S. K. Saxena, (American Society of Civil Engineers, 1979) pp. 549-564.

13. McCauley, T. V., "Planning Workovers in Wells with Fault-Damaged Casing, South Pass Block 27 Field," J. Pet. Tech., (July, 1974).

14. Yerkes, R. F. and Castle, R. O., "Seismicity and Faulting Attributable to Fluid Extraction," Eng. Geology, vol. 10, 1976, pp. 151-67.

Table 1. Sample Reservoir Parameters

Top of Formation, D	1000 ft. (305 m) dp.
Formation Thickness, H	1000 ft. (305 m)
Formation Compaction Factor, C_m	9.0 E-06/psi (1.3 E-03/MPA)
Poisson ratio, ν	0.30
Pressure Drawdown, ΔP	500 psi (3.45 MPa)

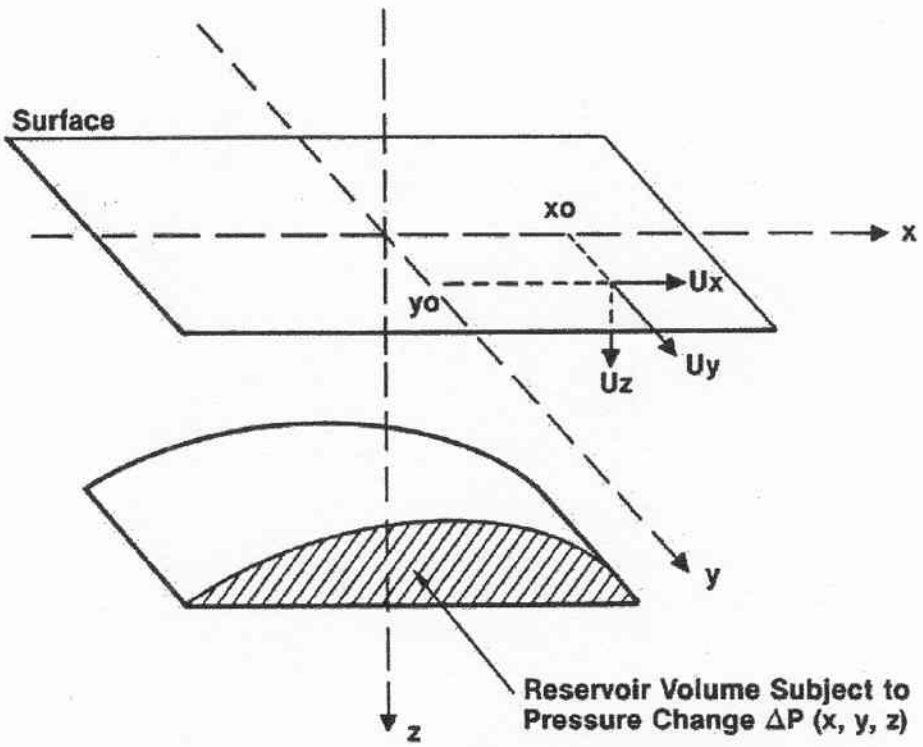

Figure 1
Surface Displacements Above a Compacting Reservoir

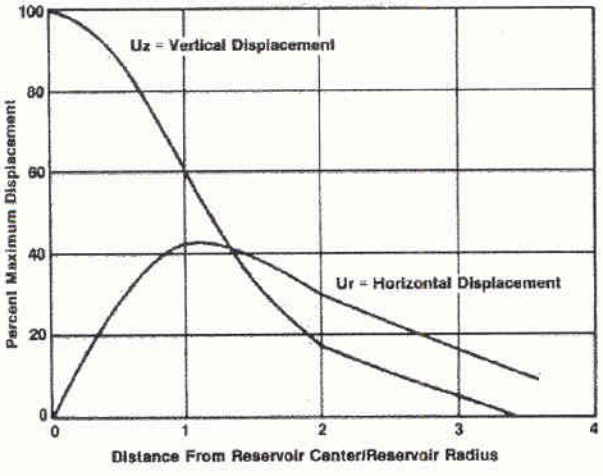

Figure 2
Subsidence Pattern Above Disk Shaped Reservoir (D/R = 1)

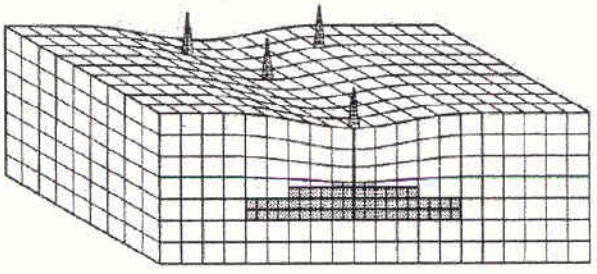

- Solves Compaction/Subsidence Eqns Numerically
- May Vary Reservoir Shape, Material Properties
- Can Solve for Non Uniform Pressure Drawdown
- Can Apply Axisymmetric, Plane Strain, or Full 3D Model
- Provides Horizontal and Vertical Displ. Throughout Field

Figure 3
Finite Element Subsidence Model

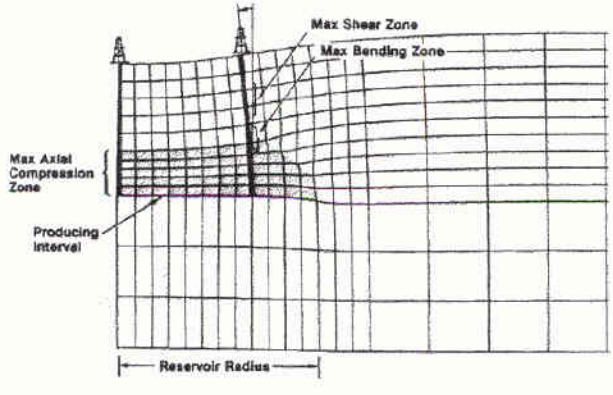

Figure 4
Potential Well Failure Locations

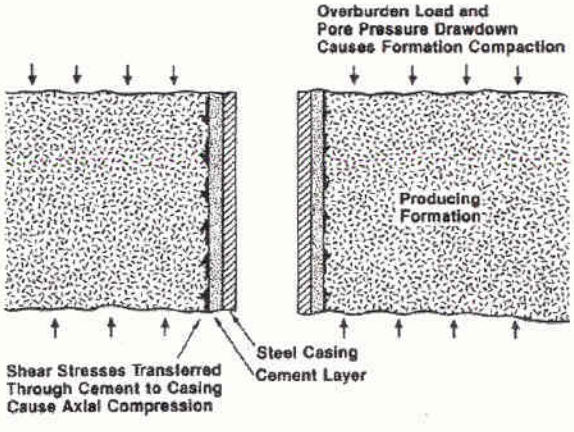

Figure 5
Typical Well Completion Subject to Formation Compaction

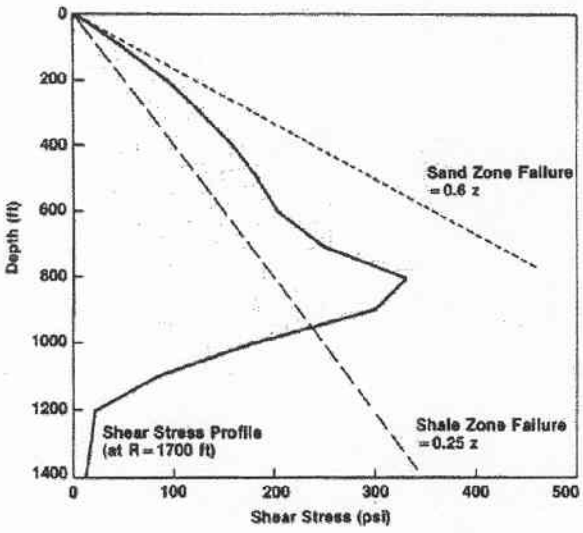

Figure 6
Shear Stress vs Depth for Sample Reservoir

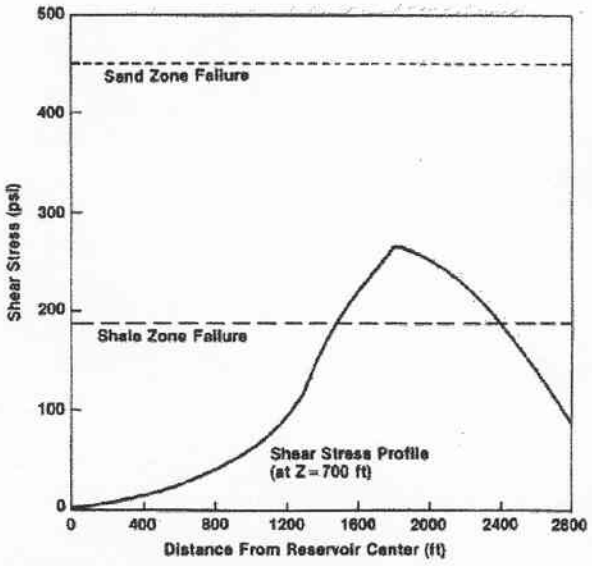

Figure 7
Shear Stress vs Lateral Position for Sample Reservoir

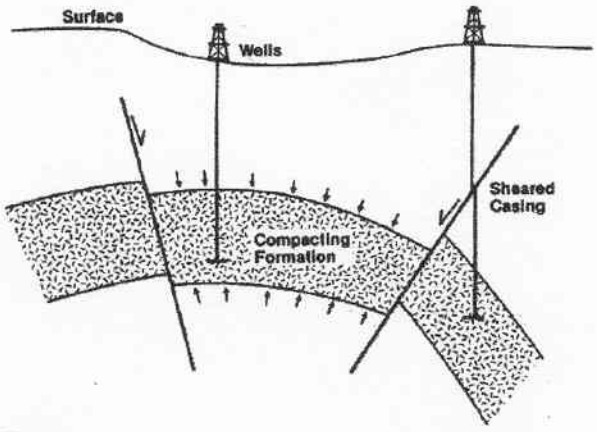

Figure 8
High Angle Faults May Be Activated by Compacting Formation